Spin dynamics of the magnetic dimer $[Fe(OMe)(dpm)_2]_2$ studied using Mössbauer spectroscopy

L. Cianchi, F. Del Giallo, M. Lantieri, and P. Moretti
Istituto di Fisica Applicata "N. Carrara," CNR, via Panciatichi 64, 50127 Firenze, Italy

G. Spina
Unità INFM di Firenze, Dipartimento di Fisica, Università di Firenze, via G. Sansone 1, 50019 Sesto Fiorentino (FI), Italy

A. Caneschi
Dipartimento di Chimica, Università di Firenze, via della Lastruccia 3, 50019 Sesto Fiorentino (FI), Italy
(Received 12 November 2002; revised manuscript received 21 August 2003; published 28 January 2004)

We present a study of the spin dynamics of the magnetic dimer $[Fe(OMe)(dpm)_2]_2$, using Mössbauer spectroscopy. In this cluster, the two iron(III) ions are antiferromagnetically coupled so that the dimer presents a $S=0$ spin ground state. Spin multiplets with values of S ranging from 1 to 5 follow in order of increasing energy. Axial anisotropy DS_z^2 is also present with D of the order of a few kelvin. Spectra were collected over a range from 6.5 K to room temperature. They consist of doublets in which any magnetic structure is lacking, but the line widths of which increase with the temperature, due to relaxation effects. We performed their fits by assuming a fast-fluctuating hyperfine field which stochastically inverts its direction along the anisotropy axis. The zero-frequency Fourier transform J_z of the hyperfine-field correlation function versus the temperature was obtained from the spectrum fittings. The trend of J_z suggests that the basic mechanisms of the spin dynamics consist of a tunnel effect due to magnetic-anisotropy transversal terms, as well as of spin-thermal bath interactions. By assuming this, the following parameters were estimated from the fitting of $J_z(T)$: $D(1)\approx 8.1$ K, $E/D(1)\approx 8.5\times 10^{-4}$, and $w=w_0\exp(-2T_0/T)$ with $w_0\approx 9.2\times 10^8$ s^{-1} and $T_0\approx 732$ K. Lastly, similarities in spin dynamics between the dimer and the ring shaped clusters were discussed.

DOI: 10.1103/PhysRevB.69.014418 PACS number(s): 67.57.Lm, 61.46.+w, 87.64.Pj

I. INTRODUCTION

Within the research field on molecular magnetic clusters, the problem concerning the nature of the basic mechanism of spin dynamics has not yet been entirely clarified. This is an important issue, both for theoretical aspects concerning the features of the spin–phonon interaction in mesoscopic systems, and also for possible applications, since spin fluctuations affect magnetization.

Experimental studies of spin fluctuations in a certain number of clusters were carried out by using magnetization measurements,[1,2] ^{1}H-NMR technique,[3–5] and, for clusters of Fe(III) magnetic ions, Mössbauer spectroscopy.[6–8] Mössbauer spectroscopy is particularly effective in studying the spin dynamics of these clusters, since probes (i.e., the ^{57}Fe nuclei) are strongly coupled, through the hyperfine interactions, with the electrons that determine the magnetic properties of the cluster. Moreover, this technique can reveal fluctuation frequency of the hyperfine field within the very wide range from 10^6 to 10^{12} s^{-1}.

In some of the above-mentioned studies, clusters with high-spin ground states were considered and correlation functions of the spin components were determined in a range of temperatures where only the ground state is important[1,2,5,7,8].

Furthermore, a family of clusters consisting of a series of even iron(III) ions in complanar ring-shaped arrangements was studied.[3,4,6] In these, contributions of the excited spin states could not be disregarded because the ground state is diamagnetic. An antiferromagnetic coupling between iron ions is present in these compounds and the cluster spin states can be fairly well described by means of an Heisenberg Hamiltonian with nearest-neighbor coupling,[9,10]

$$H=J\left(\sum_{i=1}^{N-1}\boldsymbol{S}_i\cdot\boldsymbol{S}_{i+1}+\boldsymbol{S}_N\cdot\boldsymbol{S}_1\right), \tag{1}$$

where $\boldsymbol{S}_i$ is the spin of the ith magnetic ion, N is the number of magnetic ions, and J the exchange constant. However, the J values change, depending on the type of bridging ligand, in the range from about 15 to about 30 K. A small axial anisotropy is also present with a constant of the order of a few kelvin.[11]

In such even-ion systems, antiferromagnetic coupling leads to an $S=0$ ground singlet. The singlet-triplet gap depends on the cluster composition: in any case, its order of magnitude is J.

A Mössbauer study of a ring with six iron(III) ions[6] showed that spectra from 10 to 20 K were consistent with the presence of a diamagnetic ground state $S=0$ that, in this temperature interval, made the prevalent contribution. For higher temperatures, the effect of the spin fluctuations becames more and more evident. This was because the spectrum linewidth Γ increased monotonically with increasing temperature from about 50 to 200 K, showing a flat trend from 20 to 50 K. From the trend of Γ versus temperature, a qualitative estimate of the correlation time τ of the spin components could be obtained: τ was found to increase with the temperature from 20 to 200 K. Results in agreement with the Mössbauer ones were obtained in a ^{1}H-NMR study on rings with six and ten iron(III) ions,[3] by taking into account the fact that T_1^{-1} is proportional to the Fourier transform of the

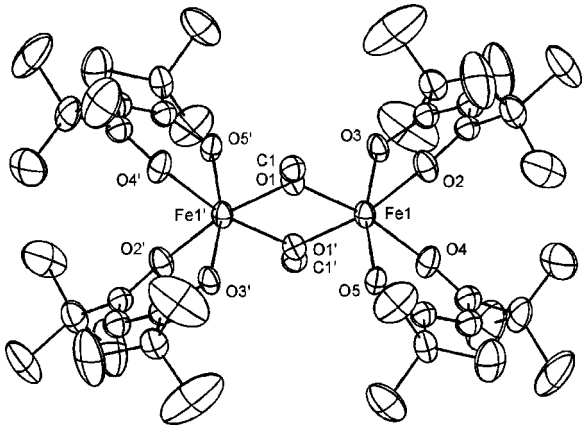

FIG. 1. ORTEP view of the complex $[Fe(OMe)(dpm)_2]_2$

correlation functions (CF) of the spin components.[3] In any case, due to the energy–level complexity, a quantitative analysis of such CF's is very cumbersome. Therefore, a different theoretical approach in terms of collective *q*-dependent spin variables, together with assumptions concerning the collective-excitation spectrum, was used.[12] In Ref. 12 the calculated trend of T_1^{-1} with temperature is found to compare fairly well with the measured one.

In the present Mössbauer study, we will investigate the spin dynamics of the $S=0$ ground-state clusters, by considering a member of this family with very simple sets of spin states, i.e. a cluster with only two antiferromagnetic-coupled Fe(III) ions; its chemical formula is $[Fe(OMe)(dpm)_2]_2$ (Fig. 1). Such a dimer has only six spin levels: the ground-state singlet $S=0$ and, in order of increasing energy, the multiplets $S=1$, 2, 3, 4, 5. Detailed structure and magnetic properties of this cluster are reported in Ref. 13.

II. EXPERIMENTAL PROCEDURE AND RESULTS

The material under examination consists of triclinic microcrystals ($P\bar{1}$ space group), the lattice sites of which are occupied by $[Fe(OMe)(dpm)_2]_2$ clusters.[13] The sample was prepared by mixing powder of the material with wax (Eicosano Aldrich, Inc.) and by compressing the mixture into a disk shape. The effective thickness of iron was 8.7 mg cm^{-2}.

The Mössbauer spectra were determined by using a conventional sinusoidal acceleration spectrometer that operated in a multichannel scaling mode. The γ-ray source, which consisted of 25 mCi of ^{57}Co in a rhodium metal matrix, was maintained at ambient temperature. A natural abundance iron foil was used to calibrate the spectrometer . A liquid-helium cryostat was used to cool the sample with temperature measurement and control based on calibrated Cernox sensor in conjunction with a Lab-View-driven instrument.

A. Preliminary analysis of the spectra

Fifteen spectra of 1024 channels in ± 6 mm s^{-1} velocity range were collected between 6.5 and 288 K (Fig. 2). In Fig. 3, a series of spectra are shown to illustrate the evolution of the spectrum shape with the temperature. Since the Fe(III) sites in the dimer are identical to each other, the two line spectra obtained are single site doublets.

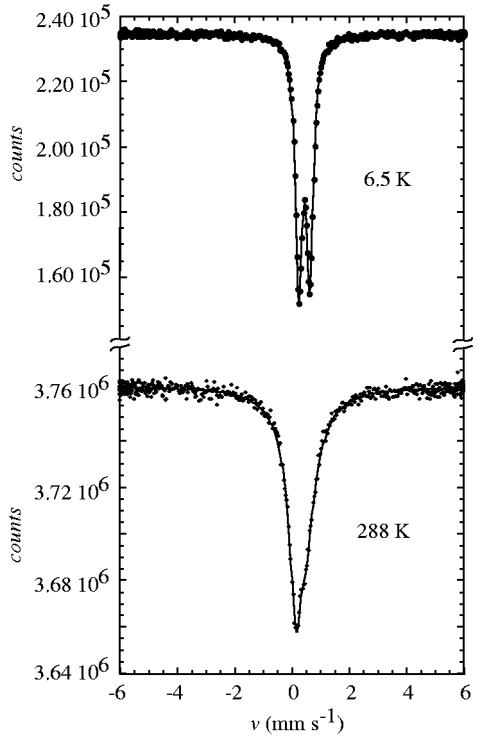

FIG. 2. Spectra collected at the 6.5-K and 288-K boundary temperatures. The solid lines represent the relative fits obtained from the model described in Sec. V.

The spectra have fairly narrow lines, and are similar for temperatures lower than about 50-60 K (low-temperature range). For $T \gtrsim 100$ K (high-temperature range) the spectrum lines become wider and wider as the temperature increases. The line broadening is much more evident for the line corresponding to the most energetic transition.

Moreover, the two lines have a slightly different peak height in *all* the spectra. In general, different peak heights can be due either to Lamb-Mössbauer *f*-factor anisotropy (Goldanskii effect),[14] to hyperfine field fluctuations (Blume effect),[15] to preferential orientations of the grains in the sample, or to more than one of these effects. In the present case the grains have regular shapes, neither flat nor needle shaped, so that we can reasonably exclude preferential grain-orientations. In order to investigate the other two effects, we considered spectra in low- and high-temperature ranges. Each of them was then fitted with two symmetrical doublets (one doublet for every line), so that the width and area of the two spectrum lines could be compared.

In Table I, for example, the fitting results for spectra at 6.5 and 150 K are reported. As far as the 6.5-K spectrum is concerned, since both Δ and Γ are, within the errors, the same for both the lines, the corresponding linewidths are equal. Instead, their absorption areas are slightly different. We also note that, since Δ is not null, the two lines do not have Lorentzian shape, but have squashed tips originating from saturation effects. However, as the lines have equal

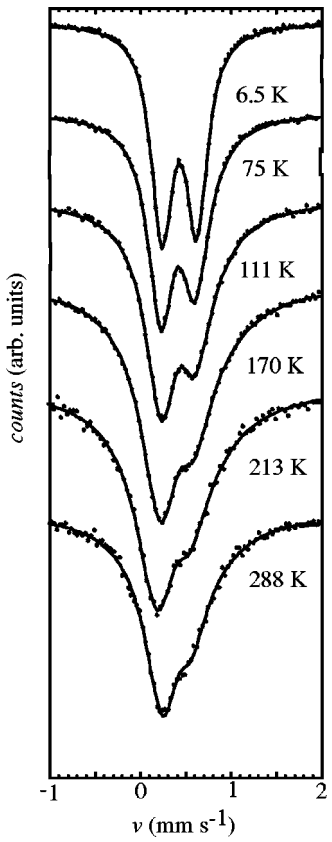

FIG. 3. Set of characteristic spectra collected in a range from 6.5 K to room temperature. Solid lines represent the relative fits obtained by the model described in Sec. V. The velocity range is restricted between -1 and 2 mm s^{-1} in order to emphasize the line shape evolution.

widths, the asymmetry of the doublet is not due to fluctuations of the hyperfine field, but rather to a small Goldanskii effect.

Conversely, in the 150-K spectrum the line corresponding to the most energetic transition (line 2) has both a smaller area and is broader than line 1. Consequently, relaxation reduces the line 2 peak height as the Goldanskii effect does. Moreover, both the lines have Lorentian shape ($\Delta \approx 0$): i.e., saturation effects are practically absent in this spectrum. We note the different broadening of the two lines, which is a typical feature of the Blume effect. Similar results were obtained for the other spectra in the low-T and high-T ranges.

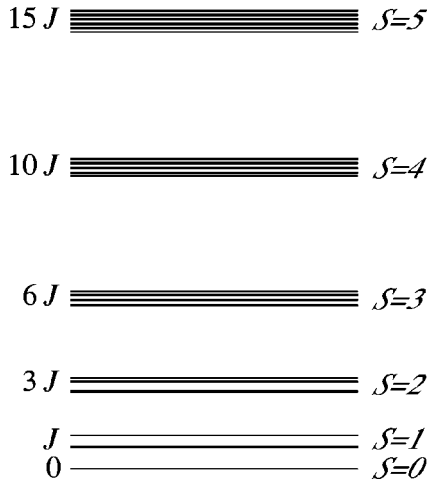

FIG. 4. Spin levels of the complex $[Fe(OMe)(dpm)_2]_2$ according to the Hamiltonian of Eq. (2).

III. THEORY OF THE SPECTRUM FITS

A. Preliminary considerations

A theoretical model for the line shape will be now described. The cluster spin states are eigenstates of the Hamiltonian[13]

$$H = J\boldsymbol{S}_1 \cdot \boldsymbol{S}_2 - DS_\zeta^2 + H_T, \tag{2}$$

where $\boldsymbol{S}_1$ and $\boldsymbol{S}_2$ are the two Fe(III)-ion spins, $S_1 = S_2 = 5/2$; J is the exchange constant, $J = 27.4$ K.[13] Moreover, S_ζ is the cluster spin component in the direction of the magnetic anisotropy. The second term on the right-hand side represents the axial magnetic anisotropy. Lastly, H_T includes high-order inner-interaction terms, as detailed in Sec. IV.

The spin states, which can be described by disregarding the H_T terms ($H_T/D \lesssim 0.01$), are indicated in Fig. 4. The ground state corresponds to $S = 0$; the spin multiplets $S = 1,2,3,4,5$ then follow in order of increasing energy.

As far as the magnetic anisotropy is concerned, it depends on single ion and dipolar contributions which are involved in different ways in different multiplets. However, electron paramagnetic resonance measurements on a similar dimer showed the single ion contribution to be widely prevalent,[16] we therefore will suppose this to be true also for our dimer. In this case the anisotropy-axis direction ζ can be assumed to

TABLE I. Fitting test relative to 6.5-K and 150-K spectra. Values of δ_{IS} (isomer shift), Δ (quadrupolar splitting), $\mathcal{A}$ (ratio between the absorption area and background), and Γ (linewidth) are obtained by fitting each line of the spectra with a doublet. The 6.5-K spectrum lines have non-Lorentian shapes of the same width and a slightly different absorption area. Instead, the 150-K spectrum line has Lorentian shapes, but different widths and areas.

		δ_{IS} (mm/s)	Δ (mm/s)	$\mathcal{A}$	Γ (mm/s)
6.5 K	line 1	0.2382(5)	0.077(3)	0.245(2)	0.218(3)
	line 2	0.6158(6)	0.076(3)	0.237(2)	0.221(3)
150 K	line 1	0.2041(3)	$<10^{-6}$	0.1105(3)	0.48(1)
	line 2	0.6098(8)	$<5\times10^{-6}$	0.0985(4)	0.66(1)

be independent of S, although this direction is not known. Moreover, the D value depends on S according to the expression:[17]

$$D(S) \propto \frac{3S(S+1)-38}{2(2S+3)(2S-1)}. \tag{3}$$

Since the spectra display no magnetic structures, we can conclude that the average of the hyperfine field in a Larmor period ($\approx$10 ns) is zero. That is, we are in the *fast relaxation limit*[18] in which contributions to the spectra of a single spin multiplet correspond to a null hyperfine field and fluctuations affect only linewidths. This means that, in order to fit the spectra, spin fluctuations can be considered as a sequence of fast inversions, $S \rightleftharpoons -S$, of the maximum value of the ζ component of the spin.

Let us now consider transitions between states of different multiplets. Until their probabilities per unit time are much smaller than the Larmor frequencies of the precession motion of the nuclear spin around the hyperfine field generated by electron spin, Mössbauer spectra are the sum of the single-multiplet contributions, all of which are weighted with the corresponding occupation probability. Conversely, if the transitions are faster than the hyperfine precessions, we can assume that the ^{57}Fe nuclei undergo a fluctuating hyperfine field corresponding to a suitable mean value of the spin.

Lastly, if the transition rates and hyperfine frequencies are comparable, spectra shapes explicitly depend on the transition probabilities between states of different multiplets. However, in this case the calculation of spectrum shapes is very complicated, since large complex non-Hermitian matrices, which contain many parameters, have to be diagonalized. As a result, long computation times are expected; moreover, great uncertainties regarding the parameter values will result from their correlations. For these reasons, two simplified models (which correspond to the limit cases mentioned above) will be used. The fitting suitability will show us the temperature ranges in which these models are valid.

B. General features of the models

In order to establish details of our models, we must know the directions of the principal axes for the elastic and EFG tensors at the iron sites and also the direction of the magnetic anisotropy axis. Since the Fe-Fe straight line is a symmetry axis of the dimer, it has to be a principal axis of both the elastic and EFG tensors. Moreover, as the Fe-bound distribution is fairly symmetrical around the Fe-Fe straight line, for the sake of simplicity we will assume that the elastic tensor has cylindrical symmetry.

As far as the EFG is concerned, a calculation based on a point charges model was carried out in which only oxygen ions nearest neighbors to the Fe(III) ions were considered. Each iron atom transfers about half an electron to each one of the six closest oxygen ions ($Fe \rightarrow Fe^{+3}$). Moreover, the two bridging oxygen atoms are bound to both the iron ions, while the other oxygen atoms are bound only to one. Lastly, we note that it is not important to set the charge values but their ratios, since we are interested only in the principal-axes directions. Consequently, we assumed a value of q_0 for the charge of the latter, and a value q_1 for the bridging oxygen atoms: a greater value, which was varied from q_0 to 2.6 q_0. From this calculation we found that one of the EFG principal axes was effectively directed along the Fe-Fe straight line, no matter how the q_1 value was. Moreover, the EFG component with respect to this axis was of a positive sign and increased with q_1. The remaining two axes were directed, one in the Fe1O1Fe1′O1′ plane (Fig. 1) and the other, perpendicularly to this plane. However, this is true for $q_1 > 1.6 q_0$; as q_1 decreases, they rotate as far as about 45° for $q_1 = q_0$.

Since both the symmetry axis of the elastic tensor and one of the principal axes of the EFG tensor are directed in the Fe-Fe direction, it is convenient to assume that the z axis (quantization axis) is in this direction. As far as the magnetic anisotropy axis is concerned, no direct experimental evidence exists regarding its direction. However, from a preliminary analysis of the spectra (Sec. II A), we noted that the line corresponding to the most energetic transition (line 2) is broader than the other one (line 1).

The relative peak heights of the two spectrum lines depend on three quantities

(1) The ratio r between the elastic-tensor components parallel and perpendicular to the z axis.

(2) The sign of V_{zz}.

(3) The orientation of the fluctuating hyperfine field with respect to the z axis. Depending on whether it is parallel or perpendicular to the z axis, we have, respectively, longitudinal or transversal relaxation.

It is easy to see that, among all the possible physical situations, only the following two fit the observed features of the spectra: (A) $r > 1$, $V_{zz} > 0$ and longitudinal relaxation and (B) $r < 1$, $V_{zz} < 0$ and transversal relaxation.

Taking the shape of the iron thermal ellipsoid into account,[13] Fig. 1, we can assume that situation (A) is satisfied. In addition, we note that our simple estimate of the EFG components gives $V_{zz} > 0$.

IV. INDEPENDENT-MULTIPLET APPROXIMATION AND RESULTS

In this approximation, spectra consist of the superposition of the contributions belonging to each one of the spin levels. In order to determine the spectrum relative to a given multiplet S, the relaxation theory in the fast relaxation limit (see, for example, Refs. 18 and 19) was used. By denoting with θ the angle between the γ-ray direction and the quantization z axis, the absorption section $\sigma(\omega)$ can be written in the form

$$\sigma(\omega) = \frac{n_a \sigma_0 \Gamma_a}{4}\left[\langle f(\theta)(1+\cos^2\theta)\rangle\left(H_{11}^{+} + \frac{1}{3}H_{22}^{+}\right) + \frac{4}{3}\langle f(\theta)(1-\cos^2\theta)\rangle H_{22}^{-}\right], \tag{4}$$

where n_a is the number of Mössbauer atoms per unit area of the sample, σ_0 is the resonant absorption section, Γ_a and $f(\theta)$ are the linewidth and the Lamb-Mössbauer factor of the absorber, respectively. Lastly, the $H-$quantities are given by:

$$H_{11}^{+}=\frac{G_{12}^{2}G_{22}^{+}+G_{11}^{+}[G_{22}^{+2}+(\omega+\omega_1)^2]}{[G_{11}^{+}(\omega+\omega_1)+G_{22}^{+}(\omega-\omega_1)]^2+(G_{12}^{2}+G_{11}^{+}G_{22}^{+}-\omega^2+\omega_1^2)^2},$$

$$H_{22}^{\pm}=\frac{G_{12}^{2}G_{11}^{\pm}+G_{22}^{\pm}[G_{11}^{\pm 2}+(\omega-\omega_1)^2]}{[G_{11}^{\pm}(\omega+\omega_1)+G_{22}^{\pm}(\omega-\omega_1)]^2+(G_{12}^{2}+G_{11}^{\pm}G_{22}^{\pm}-\omega^2+\omega_1^2)^2}, \tag{5}$$

where

$$G_{11}^{\pm}\equiv\frac{J_z}{4}(3g_1\mp g_0)^2+\frac{\Gamma_a}{2}, \tag{6}$$

$$G_{22}^{\pm}\equiv\frac{J_z}{4}(g_1\pm g_0)^2+\frac{\Gamma_a}{2}, \tag{7}$$

$$G_{12}\equiv\frac{e^2qQ}{4}\frac{\eta}{\sqrt{3}}, \tag{8}$$

$$\omega_1\equiv\frac{e^2qQ}{4}, \tag{9}$$

where J_z is proportional to the Fourier transform of the hyperfine-field correlation function. To be more precise, J_z is defined by

$$J_z=\mu_N^2\int_0^\infty\langle B_{hy}(0)B_{hy}(t)\rangle dt. \tag{10}$$

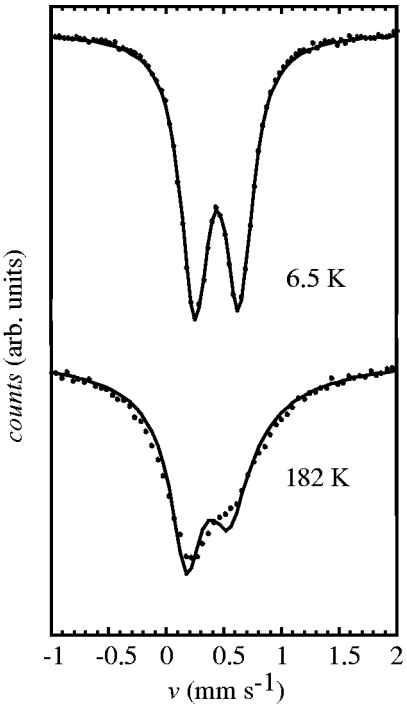

FIG. 5. Spectra at 6.5 K and 182 K and relative fits (solid lines) obtained by the independent multiplets model.

Moreover, $g_0=0.180$ and $g_1=-0.103$ are the gyromagnetic factors of the ground and the excited Mössbauer levels, respectively, $q=V_{zz}/|e|$, and η is the asymmetry parameter. Since we chose the z axis along the Fe-Fe direction, regardless of whether or not V_{zz} is the maximum component of EFG, $\eta>1$ values are possible.

As far as the hyperfine field is concerned, if the cluster is in the level S, the maximum z component of the Fe(III)-ion spin is $S/2$. Therefore, by denoting the hyperfine field corresponding to $S_z=5/2$ with B_{max}, $B_{\rm hy}$ will be given by

$$B_{\rm hy}=\frac{S}{5}B_{max}. \tag{11}$$

The spectrum expressions of the multiplets times the relative occupation probabilities were totaled and the average with respect to θ was carried out.

In order to take saturation effects into account, spectra were obtained by transmission integral method.[20] Moreover, a Voigt profile was used for the line shape of the source.[21]

The results obtained by means of the independent-multiplet model are satisfactory only for temperatures lower than about 50 K. For higher temperatures, fits are more and more unsatisfactory as the temperature increases. For example, $\chi^2=1180$ was obtained in the 6.5-K spectrum fitting, while in the 182-K spectrum fitting we obtained $\chi^2\approx 1600$. We note (Fig. 5) that, in the calculated 182-K spectrum, the double-line shape is still very present. This is mainly due to the contribution of the $S=0$ state. Conversely, in the experimental spectrum, lines are much more enlarged. This means that transitions between states of different multiplets cannot be disregarded at high temperatures. Therefore, the second fitting model was considered: in it these transitions are much faster than the Larmor precession.

V. MEAN-SPIN APPROXIMATION AND RESULTS

In this model, Mössbauer spectra are given by the equations of Sec. IV in which the J_z parameter is related to a suitable mean value of the cluster spin (see Sec. III A). Very good fits were obtained at all temperatures (Fig. 3), with χ^2 values varying between 980 and 1160. It is therefore worthwhile analyzing the values of the parameters and their trends.

Quadrupolar parameters. The quadrupolar splitting Δ shows casual variations of an order of 5%; it can be therefore considered independent of the temperature and its variations can be bound to statistical effects. We then obtain $\Delta=0.38\pm 0.01$ mm s^{-1}. As far as the symmetry parameter is concerned, apart from the 6.5-K spectrum fit, which was unaf-

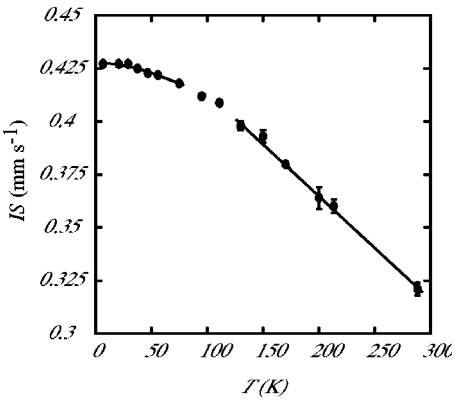

FIG. 6. Trend of IS vs *T*. High-*T* and low-*T* best-fit lines are also indicated (see text).

fected by variations of this parameter, the best fits of the other spectra gave $\eta \approx 4$. That is, the *z* axis corresponds to the smallest component of the EFG tensor.

Isomer shift. The observed monotone reduction in the isomer shift as the temperature increases (Fig. 6) is nothing more than the effect of the thermal atomic motion (second-order Doppler effect).

A cluster with *N* atoms has $3N$ freedom degrees, three of which correspond to translations and three to rotations of the whole molecule. But clusters occupy sites of a crystal lattice, so that these whole motions are in fact true oscillations. The latter, however, have low frequencies, since the oscillating masses are large and the interactions between clusters are very small due to the large site interdistances.

By denoting the normal coordinates of the cluster with $Q_\alpha(\alpha=1,\ldots,3N)$ and the *i*th displacement component of an iron ion with $u_0^{(i)}(i=x,y,z)$, we have

$$u_0^{(i)} = \frac{1}{M} \sum_{\alpha=1}^{3N} S_{0,\alpha}^{(i)} Q_\alpha , \tag{12}$$

where *M* is the mass of the iron ions and *S* is a suitable unitary matrix[22] of order $3N$, so that $\Sigma_{\alpha=1}^{3N} S_{0,\alpha}^{(i)} \tilde{S}_{\alpha,0}^{(i)} = 1$. The mean-square velocity of the iron ions is then given by

$$\langle v^2 \rangle = \frac{\hbar}{2M} \sum_{\alpha=1}^{3N} \sum_{i}^{x,y,z} \omega_\alpha \coth\left(\frac{\hbar\omega_\alpha}{2k_B T}\right) (S_{0,\alpha}^{(i)})^2 . \tag{13}$$

For $T \gg \hbar\omega_{\max}/k_B$, where $\omega_{\max}$ denotes the maximum of the mode frequencies, the classical limit is obtained from:

$$\langle v^2 \rangle = \frac{3k_B T}{M} . \tag{14}$$

Thus, at high temperatures IS should follow the classical trend:[14] $\delta_{IS} = \text{const} - 3k_B T/2Mc$. *M* is the ^{57}Fe mass, so that: $3k_B/2Mc = 7.3\,10^{-4} \text{mm s}^{-1} K^{-1}$. Indeed, we can see (Fig. 6) that the experimental data show a linear trend for temperatures higher than 100 K. In this range, we obtained $\delta_{IS} = (0.46 - -5.0\times10^{-4} T)\text{mm s}^{-1}$. That is, the *T* coefficient is about 70% of the one given by the classical limit. A qualitatively similar result was obtained in a high-temperature IS analysis of Ce-filled antimonide skutterudites,[23] and was attributed to the fact that the temperature range analyzed was not high enough.[24]

Here as follows, we will discuss the previous result by using a molecular approach, rather than a crystalline-solid one. Let us divide the terms of the sum in Eq. (13) into low frequency terms ($\hbar\omega/k_B < 100K$) and high-frequency terms (the other ones). We can then rewrite Eq. (13) (for $T > 100$ K) as

$$\langle v^2 \rangle \approx \frac{k_B T}{M} \sum_{\alpha=1}^{l} \sum_{i}^{x,y,z} (S_{0,\alpha}^{(i)})^2 + \frac{\hbar}{2M} \sum_{\alpha=l+1}^{3N} \sum_{i}^{x,y,z} \omega_\alpha \coth\left(\frac{\hbar\omega_\alpha}{2k_B T}\right) (S_{0,\alpha}^{(i)})^2 , \tag{15}$$

where *l* denotes the mode of the first set with the highest frequency. Since the IS data for 100 K$<T<$300 K follow a linear trend, the second term on the right-hand side of Eq. (15) must be constant within this same temperature range. In other words, for the high frequencies set $\coth(\hbar\omega_\alpha/2k_B T) \approx 1$. Apart from a constant term, we thus obtain:

$$\langle v^2 \rangle \approx \frac{k_B T}{M} \sum_{\alpha=1}^{l} \sum_{i}^{x,y,z} (S_{0,\alpha}^{(i)})^2 . \tag{16}$$

As mentioned above, the IS linear fit leads to $\Sigma_{\alpha=1}^{l} (S_{0,\alpha}^{(i)})^2 \approx 0.7$, instead of 1. This means that 70% of the vibrational energy of the iron ions is related to low-frequency modes. That is, the high-frequency modes slightly involve the iron ions. This is obvious enough, as among the cluster atoms the iron ions have the largest mass. Moreover, we note that a large gap separates the low-frequency set from the high-frequency one. In fact, as far as the former set is concerned, it has to be $\hbar\omega/k_B T \lesssim 100$ K and, with regard to the latter, $\hbar\omega/k_B T \gtrsim 300$ K.

We can also obtain an estimate of the mean frequency for the low-frequency set by fitting the low-temperature δ data. In fact, for low temperature, the decrease in δ with the temperature is slow. It is possible to verify by means of numerical calculations that, for a certain mode distribution, its trend can be simulated with good approximation by supposing that all the modes have a same suitable mean frequency Ω. By fitting the IS data in the low temperature range with a function having the form $\delta_{IS} = \delta_0 - \hbar\Omega/4Mc \coth(\hbar\Omega/2k_B T)$, we obtain an estimate of Ω. For data in the $T<80$ K range, the best fit of IS (Fig. 6) is obtained for $\Omega = (1.19 \pm 0.09) \times 10^{13} \text{s}^{-1} \equiv 91$ K and equivalent values are obtained for lower temperatures. For example, values of Ω of $(1.18 \pm 0.1) \times 10^{13}$ s^{-1} and $(1.14 \pm 0.2) \times 10^{13}$ s^{-1} are obtained for $T<60$ K and $T<50$ K, respectively.

Goldanskii parameter. Let us consider the quantity $a = k^2(\langle z^2 \rangle - \langle x^2 \rangle)$, where *k* is the γ-ray wave number and $\langle z^2 \rangle$ and $\langle x^2 \rangle$ are, respectively, the mean-square displacements along the quantization axis and perpendicular to it. As can be shown by a straightforward calculation, *a* is connected with the ratio R_G of the spectrum-line intensities through the relation:

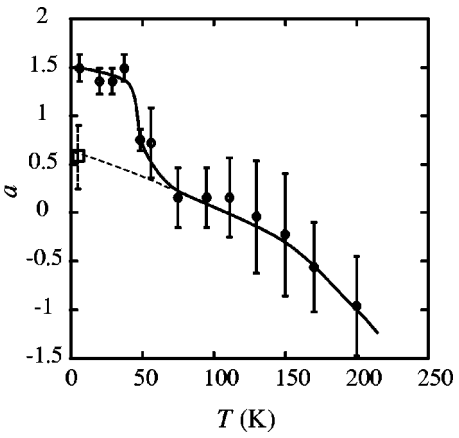

FIG. 7. a values obtained from the spectrum fits using the mean-spin model. Data for $T>200$ K are not indicated, because the spectrum fits were not very sensitive to the a value. The a value of 0.53 ± 0.3 at $T=6.5$ K was obtained from the ratio of the $\mathcal{A}$ values of Table I. The solid and broken lines are a visual guide.

$$R_G=\frac{4(\eta^2+3)^{1/2}+\dfrac{\displaystyle\int_0^1\sqrt{3}(3\xi^2-1)\exp(-a\xi^2)d\xi}{\displaystyle\int_0^1\exp(-a\xi^2)d\xi}}{4(\eta^2+3)^{1/2}-\dfrac{\displaystyle\int_0^1\sqrt{3}(3\xi^2-1)\exp(-a\xi^2)d\xi}{\displaystyle\int_0^1\exp(-a\xi^2)d\xi}}, \tag{17}$$

where $\xi=\cos\theta$.

The values of R_G were obtained from the spectrum fits. From these, we could obtain the corresponding a values by means of a numerical inversion of Eq. (17). The trend of a versus T is shown in Fig. 7. In this figure, the a value at $T=6.5$ K directly obtained from the ratio of the areas of the two lines (Table I) by assuming $\eta=4$ is also reported. As can be seen, the latter is much smaller than the values obtained for $T<40$ K through the mean spin model. These high low-temperature a values, together with the sudden decreases from 40 to 70 K, are due to the inadequacy of the mean spin model for fitting the low-temperature spectra, as we will discuss in detail in Sec. VI.

We note that a as a function of T would seem to change sign for temperatures higher than about 130 K, i.e., the oscillation amplitude of the iron ions along z would become smaller than the one along x. However, our data are not definitive. In fact, the a values for $T<130$ K are positive, but near to zero, apart from the 6.5 K value, so that, taking the error bars into account, small negative values are also possible. Moreover, since the fitting of the 6.5-K spectrum is unaffected by the changing in the η parameter, in order to evaluate the a value at $T=6.5$ K we assumed the value of η which was obtained at higher temperatures, i.e., $\eta=4$. On the other hand, η could depend on the temperature and, since smaller values of a are obtained from smaller values of η, the value $a\approx0.5$ calculated for $T=6.5$ K could be overestimated. However, if a change of the a sign is most unlikely for an usual crystalline solid as atoms move in harmonic potentials, in complex molecules, such as clusters, it could be likely that non-parabolic-shaped potentials are present, so that a change of the a sign would be evidently possible. However, these are only hypotheses, which cannot be proved from the data of the present work, further theoretical and experimental analyses being necessary.

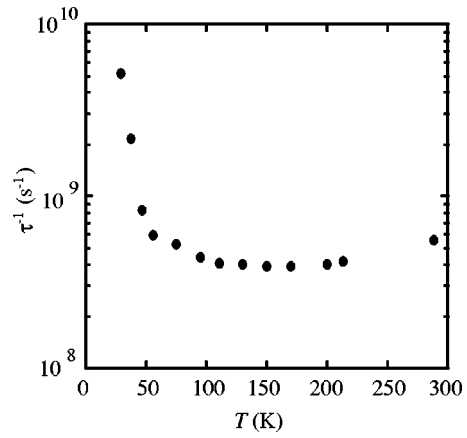

FIG. 8. τ^{-1} values obtained from the spectrum fittings by using the mean-spin model.

Relaxation parameters. As we showed in Sec. IV, spin dynamics causes the spectrum lines to be broadened by quantities proportional to

$$J_z=\int_0^\infty\langle h_z(0)h_z(t)\rangle dt=\left(\frac{\mu_N B_{max}}{5h}\right)^2\int_0^\infty\langle S_z(0)S_z(t)\rangle dt, \tag{18}$$

which, in this form, is expressed in frequency units. It is usually assumed that $\langle S_z(0)S_z(t)\rangle$ has a decreasing exponential trend: $\langle S_z(0)S_z(t)\rangle=\langle S^2\rangle\exp(-t/\tau)$, where $\langle S^2\rangle$ is the thermal mean of the square component of the spin along z. By assuming this trend, we obtain

$$J_z=\left(\frac{\mu_N B_{max}}{5h}\right)^2\langle S^2\rangle\tau. \tag{19}$$

Figure 8 shows τ^{-1} values obtained from the spectrum fittings. The values for 6.5 and 20.5 K are not considered since good fits were obtained as long as $J_z<10^4$ s^{-1} no matter what the value of this parameter was.

We can see that, as the temperature increases up to about 60 K, τ^{-1} quickly decreases. For higher temperatures, τ^{-1} shows a quasiflat trend with a slight increase for $T>200$ K.

The very high values of τ^{-1} and its steep decrease at temperatures lower than 60 K do not have a physical explanation. Therefore, this fact denotes a substantial inadequacy on the part of the fitting model to fit the spectra at $T<60$ K. The inadequacy of the mean-spin model is also correlated to the steep decrease in the a parameter, from 40 to 70 K (see Fig. 7).

The inadequacies of the theory in the low-temperature range can be explained as follows. Transitions between multiplet states slow down as the temperature decreases. Therefore, spectra will tend to become a superposition of independent single-multiplet contributions. Moreover, the contribution of the $S=0$ singlet (obviously not affected by hyperfine interaction) becomes increasingly important as the temperature decreases, so that the whole spectrum has to approach a sharp single doublet. Since in the fast relaxation limit, linewidths decrease as τ^{-1} increases[15] and, moreover, the linewidths in our spectra become smaller and smaller as the temperature become lower, the fitting model compels τ^{-1} to increase as T decreases. Furthermore, if τ^{-1} increases, the asymmetry of the two spectral lines, due to the relaxation effect, tends to be lacking. Therefore, to compensate for this, the fitting procedure increases the a parameter.

VI. ANALYSIS OF THE SPIN DYNAMICS

In the preceding section, a decreasing exponential trend for the CF of S_z was assumed. This is a phenomenological approach which is useful for obtaining qualitative information on spin dynamics. Here as follows, a more detailed analysis will be made of the CF in terms of the physical quantities characterizing the spin states.

Two causes can be invoked in order to explain the inversions in the hyperfine field: one is the interaction between spin and thermal bath, and the other is the *quantum tunnel effect*[25] (QT). In the first case, transitions between the two states of a doublet $|S,\pm M\rangle$ are related to atomic motions so that the corresponding probability per unit time $w_M^{(S)}$ depends on temperature. In the second case, the two states $|S,\pm M\rangle$ are coupled by inner interactions: for example, small terms of transverse magnetic anisotropy. Such interactions give rise to coherent transitions with independent temperature frequencies. Although QT is usually important only at very low temperatures, the flat trend of τ suggests that it may also have a role at moderate temperatures in the spin dynamics of the dimer.

For the sake of simplicity, we assumed that the basic spin Hamiltonian coupling the $|S,\pm M\rangle$ states has the lowest order in the spin components: $H_T=E(S_+^2+S_-^2)$, where E is the coupling parameter. As far as the dependence of E on S is concerned, we have no theoretical or experimental reference, since here H_T has to be considered as a pure phenomenological Hamiltonian. From this point of view, we can assume E to be independent of S.

By following the perturbative procedure which was used in Ref. 8, we obtained the tunneling frequency relative to the transitions $|S,M\rangle \rightleftharpoons |S,-M\rangle$, which is given by

$$\nu_M^{(S)}=F_M^{(S)}\left(\frac{E}{D(S)}\right)^M D(S), \tag{20}$$

where $F_M^{(S)}$ are numerical factors that depend on S and M.

Let us now determine the CF of the spin component S_z,

$$\langle S_z(0)S_z(t)\rangle=\mathrm{Tr}\{\rho S_z(0)S_z(t)\}_{c,s}, \tag{21}$$

where $\{\cdots\}_{\{c,s\}}$ means that the trace is calculated on a complete set of states of the cluster+surrounding system, and ρ is the density operator. The contribution of the doublet $|S,\pm M\rangle$ to the CF can be evaluated by means of the procedure described in the appendix of Ref. 8. We obtain

$$\langle S_z(0)S_z(t)\rangle_{S,M}=M^2\exp(-2w_M^{(S)}t)\cos(2\pi\nu_M^{(S)}t). \tag{22}$$

Lastly, the CF was obtained from the thermal mean of all the doublet contributions:

$$\langle S_z(0)S_z(t)\rangle=2\sum_{S=1}^{5}\frac{W_S}{2S+1}\sum_{M=1}^{S}M^2\exp(-2w_M^{(S)}t)\times\cos(2\pi\nu_M^{(S)}t), \tag{23}$$

where W_S is the occupation probability of the S multiplet. Obviously, the fitting of J_z did not make it possible to obtain the 15 transition probabilities $w_M^{(S)}$ and their dependencies on the temperature. We will therefore replace these quantities with their appropriate mean w value.

Since a dependency of τ on T is evident only for $T>200$ K, we can assume that the transitions due to the interaction between spin and thermal bath have to be at least of the second order. Furthermore, there are not other spin states with the same electronic configuration in addition to the spin multiplets considered. It is therefore reasonable to suppose that the basic process consists of a first-order Raman effect.[26] We also suppose that only modes of a narrow band involving the bridging oxygen atoms and the other atoms that are near neighbors to iron ions are important. Therefore, for a narrow band around k_BT_0, w has the form $w=w_0\exp(-2T_0/T)$.

We also note that the Mössbauer excited level has a finite mean life τ_M, the inverse of which could be comparable with w. Therefore, in summary, we write the CF in the form

$$\langle S_z(0)S_z(t)\rangle=2\exp[-2w't]\sum_{S=1}^{5}\frac{W_S}{2S+1}\times\sum_{M=1}^{S}M^2\cos(2\pi\nu_M^{(S)}t), \tag{24}$$

where $w'=w+\tau_M^{-1}/2$.

By replacing the right-hand side of Eq. (24) in Eq. (18), we obtain

$$J_z=\left(\frac{\mu_N B_{max}}{5h}\right)^2\sum_{S=1}^{5}\frac{W_S}{2S+1}\sum_{M=1}^{S}M^2\frac{w'}{w'^2+(2\pi\nu_M^{(S)})^2}. \tag{25}$$

A. Fitting results and conclusions

In Fig. 9 are indicated the experimental values of J_z, together with the best fit obtained from Eq. (25). We see that the latter does not give a good fitting for $T<60$ K. This fact confirms the inadequacy of the mean–spin model for the low temperature range.

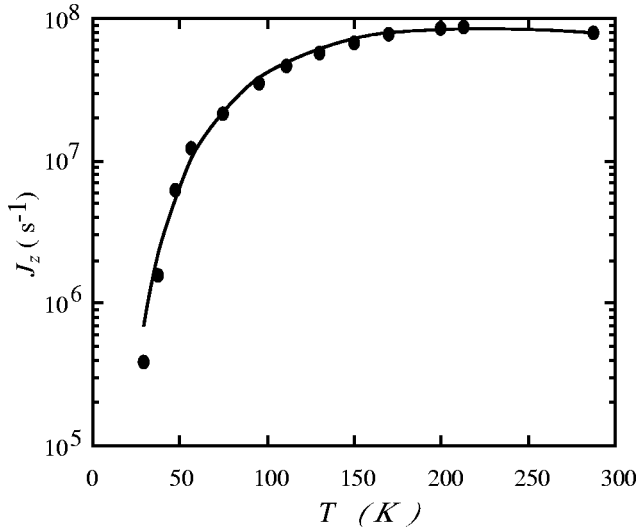

FIG. 9. Full circles denote J_z experimental values obtained from the spectrum fittings by using the mean-spin model. The solid line is the best fit obtained from Eq. (25).

The corresponding values of the parameters are shown in Table II. We included τ_M in the fitting parameters in order to check the foundation of Eq. (25). The outlet value of 0.77×10^{-7} s is of the same order of magnitude as the value reported in the literature.[14] Thus, in spite of the approximations used, we were able to obtain a reliable estimate of the parameters.

The value of 732 K for T_0, which corresponds to modes of circular frequency $\omega_0 = 8.5 \times 10^{13}$ s^{-1}, could be related to modes belonging to the high-frequency band. As far as the values of $D(1)$ and $E/D(1)$ are concerned, these are substantially in agreement with EPR measurement on a similar dimer.[16] The corresponding tunneling frequencies of the multiplets are of the order of 10^9 s^{-1}, i.e., of the same order of magnitude of w_0.

(1) The good fits obtained in the high-temperature range ($T \gtrsim 90$ K) provide support to our assumption of a $V_{zz} > 0$ in the presence of fast longitudinal relaxation. This result enables us to argue that the anisotropy axis is approximately in the Fe-Fe direction, i.e. coincident with both the EFG principal axis of minimum component and the symmetry axis of the elastic tensor at the iron site.

TABLE II. Values of D and E/D for the triplet ($S=1$), τ_M, w_0, and T_0 obtained from the fitting of J_z by Eq. (25).

D (K)	$E/D(10^{-4})$	τ_M (10^{-7} s)	w_0 (10^8 s^{-1})	T_0 (K)
8.1	8.5	0.77	9.2	732

(2) As far as the spin dynamics trend with T is concerned, it can be summarized as follows. In the low-temperature range ($T \lesssim 60$ K), the main contribution to Mössbauer spectra comes from the singlet $S=0$, so that only small relaxation effects are present. As the temperature increases, multiplets with higher spin become more and more populated, and fast–relaxation effects for $T \gtrsim 90$ K are observed with spin fluctuation frequencies of order of the 10^9 s^{-1}. These frequencies are practically independent of the temperature up to about 200 K, and must be attributed to QT. Above 200 K, transitions due to interactions with the thermal bath appear, causing an increase of the spin-fluctuation frequency with the temperature.

(3) As mentioned in the Introduction, a quasiflat part of the trend of the spin-fluctuation rate versus temperature—i.e., spin-fluctuation frequency independent of T—is also present in the ring-shaped clusters, although in different ranges of temperatures for different clusters (for example, from ≈ 20 to ≈ 70 K in the Fe_6 cluster,[3,6] and from ≈ 30 k to ≈ 100 K in the Fe_{10} cluster[3]). Similarly, as the temperature increases, the spin fluctuations for all these clusters become faster and faster. We can therefore conclude that the interpretation of the spin fluctuation described in the present work can probably be used also as a model for analyzing the magnetic fluctuations of the ring-shaped clusters.

ACKNOWLEDGMENTS

We wish to acknowledge Dr. R. Sessoli and Dr. A. Cornia for useful discussions and criticisms.

[1] R. Sessoli, D. Gatteschi, A. Caneschi, and M.A. Novak, Nature (London) **365**, 141 (1993).
[2] W. Wernsdorfer, A. Caneschi, R. Sessoli, D. Gatteschi, A. Cornia, V. Villar, and C. Paulsen, Phys. Rev. Lett. **84**, 2965 (2000).
[3] A. Lascialfari, D. Gatteschi, F. Borsa, and A. Cornia, Phys. Rev. B **55**, 14 341 (1997).
[4] A. Lascialfari, Z.H. Jang, F. Borsa, D. Gatteschi, and A. Cornia, J. Appl. Phys. **83**, 6946 (1998).
[5] Y. Furukawa, K. Kumagai, A. Lascialfari, S. Aldovandri, F. Borsa, R. Sessoli, and D. Gatteschi, Phys. Rev. B **64**, 094439 (2001).
[6] A. Caneschi, M. Capaccioli, L. Cianchi, F. Del Giallo, D. Gatteschi, P. Moretti, F. Pieralli, and G. Spina, Hyperfine Interact. **116**, 215 (1998).
[7] A. Caneschi, L. Cianchi, A. Cornia, F. Del Giallo, F. Pieralli, and G. Spina, J. Phys.: Condens. Matter **11**, 3395 (1999).
[8] L. Cianchi, F. Del Giallo, G. Spina, W. Reiff, and A. Caneschi, Phys. Rev. B **65**, 064415 (2002).
[9] A. Caneschi, A. Cornia, and S.J. Lippard, Angew. Chem., Int. Ed. Engl. **34**, 467 (1995).
[10] A. Caneschi, A. Cornia, A.C. Fabretti, S. Foner, D. Gatteschi, R. Grandi, and L. Schenetti, Chem.-Eur. J. **2**, 1379 (1996).
[11] A. Caneschi, D. Gatteschi, C. Sangregorio, R. Sessoli, L. Sorace, A. Cornia, M.A. Novak, C. Paulsen, and W. Wernsdorfer, J. Magn. Magn. Mater. **200**, 182 (1999).
[12] A. Lascialfari, D. Gatteschi, A. Cornia, U. Balucani, M.G. Pini, and A. Rettori, Phys. Rev. B **57**, 1115 (1998).
[13] F. Le Gall, F. Fabrizzi de Biani, A. Caneschi, P. Cinelli, A. Cornia, A.C. Fabretti, and D. Gatteschi, Inorg. Chim. Acta **262**, 123 (1997).

[14] C. Janot, *L'effet Mössbauer et ses Applications* (Masson et C^{ie}, Paris, 1972).
[15] M. Blume, Phys. Rev. Lett. **14**, 96 (1965).
[16] E. Goovaerts, M. Stefan, P. ter Heerdt, A. Bouwen, A. Cornia, A. Caneschi, and D. Gatteschi (unpublished).
[17] A. Cornia (private communication), acornia@unimo.it
[18] See for example, L. Cianchi, M. Mancini, P. Moretti, and G. Spina, Rep. Prog. Phys. **49**, 1243 (1986).
[19] A.M. Afanasev and V.D. Gorobchenko, Zh. Eksp. Teor. Fiz. **66**, 1406 (1974) [Sov. Phys. JETP **39**, 690 (1974)].
[20] See, for example, G. Pedrazzi, in *Elements of Mössbauer Spectroscopy*, Proceedings of First National School on Mössbauer Spectroscopy, edited by G. Principi and A. Perin (CLEUP, Padova, 1998).
[21] D.G. Rancourt, and J.Y. Ping, Nucl. Instrum. Methods Phys. Res. B **58**, 85 (1991).
[22] E.B. Wilson, J.C. Decius, and P.C. Cross, *Molecular Vibrations* (McGraw-Hill, New York, 1955).
[23] G.J. Long, D. Hautot, F. Grandjean, D.T. Morelli, and G.P. Meisner, Phys. Rev. B **60**, 7410 (1999).
[24] H.R. Rechenberg, Phys. Rev. B **62**, 6827 (2000).
[25] C. Paulsen and J.-G. Park, in *Quantum Tunneling of Magnetization*, edited by L. Gunther and B. Barbara (Kluwer Academic, Dordrecht, 1995).
[26] A. Abragam, and B. Bleaney, *Electron Paramagnetic Resonance of Transition Ions* (Dover, New York, 1970).